# SWITCHING FREQUENCY MODULATION FOR MAXIMUM POWER POINT TRACKING TECHNIQUE OF PHOTOVOLTAIC SYSTEMS

BY

DAMIAN B. N NNADI, MARCEL U. AGU AND LINUS U. ANIH
Department of Electrical Engineering, University of Nigeria, Nsukka

## ABSTRACT

*This paper presents a maximum power point tracking technique using switching frequency modulation. The solar panel is connected to dc-dc converter which either may be Ćuk or SEPIC converter operating in discontinuous inductor current mode.*

*A small-signal sinusoidal perturbation is injected into the switching frequency and the result is compared with the average value of the panel terminal voltage and the ac components variation of the input voltage. With this procedure the maximum power point can then be located. Simulation results were given to validate the accuracy of the analysis.*

*Index Terms:* - **dc-dc converter, maximum power point, photovoltaic, switching frequency modulation, discontinuous inductor current mode**

## 1.0. INTRODUCTION

Energy is one of the most basic and essential of all the natural resources given to man. Sun is the bedrock of all the energy used in this planet; the energy originating from either fission or fusion of atomic nuclei in the sun. Energy released from the sun if properly harnessed will go a long way in ameliorating the world energy problems.

It is worthy to note that for ages the world energy sources depend on conventional sources such as fossil fuel, hydro, coal, radioactive decay etc.

But all these have their peculiar problems of scarcity, rapidly depleting, causing pollution which is harmful to both man and other living organisms. It is an attempt to solve the above problems that necessitated this research work. Since renewable energy sources are clean, pollution-free, harmless, recyclable, distributed throughout the earth and inexhaustible it will be a good substitute. Researches on the photovoltaic (PV) power generation have received much attention, particularly on many terrestrial applications [1]. Solar energy is directly converted into electrical energy by solar photovoltaic (PV) module. But there are still two principal barriers for the use of PV energy: the high installation cost and the low energy conversion efficiency.

The main reasons for the low electrical efficiency of PV array are the nonlinear variation of output power with solar radiation levels, operating temperature, aging and load current.

However, the nonlinear nature of PV system is apparent from Fig. 1, i.e. the current and power of the PV array depends on the array terminal operating voltage. In addition, the maximum power point varies with insolation level and temperature.

In practice, there are three possible approaches for maximizing the solar power extraction in medium- and large-scale systems. They are sun tracking and maximum power point tracking (MPPT) or both. For small-scale systems, MPPT is popular for economical reasons.

In the last two decades, various techniques have been developed for MPPT. These include perturb-and-observe method [2]. Although, it is easy to implement in its basic form, however, it has some limitations, like oscillations around the MPP in steady state operation, slow response speed, and even tracking in wrong way under rapidly changing atmospheric conditions [2].Similarly, we have Incremental Conductance (INC) method [3]. This method uses the PV array's incremental conductance di/dv to compute the sign of dp/dv (ratio of incremental power to incremental voltage). It does this using an expression derived from the condition that at MPP, dp/dv =0. Beginning with this condition, it is possible to show that, at MPP, di/dv = -i/v. Thus, INC can be determined if the tracker has reached the MPP and stop perturbing the operating point. Other methods include; voltage and current based MPPT method [4], fractional open-circuit voltage [5], fuzzy logic method [6] etc, had been proffered.

But for this research, investigations have been carried out on MPPT using a SEPIC (Single Ended Primary Inductor Converter) or Cúrk converter [7] and switching frequency modulation for PV panels [8]. These are utilized for efficiently maximizing the output power of a solar panel supplying to a load or battery bus under varying meteorological conditions. The proposed MPPT is achieved by connecting a pulse-width-modulated (PWM) dc/dc Cúrk or SEPIC converter between a solar panel and a load or battery bus. The converter is operating in discontinuous inductor current mode (DICM). These two types of converters were found to have the input resistance characteristics being proportional or inversely proportional to the switching frequency. The nominal duty cycle of the main switch ***d*** in the converter is adjusted to a certain value, so that the input resistance of the converter is equal to the equivalent output resistance of the solar panel. This ensures the maximum power transfer. By modulating a small-signal sinusoidal perturbation into the duty cycle of the main switch and comparing the maximum variation in the input voltage and the voltage stress of the main switch, the MPP of the panel can be located. In this paper the proposed technique is investigated using Simplorer 6.0 Student Version package, and the results of the simulations confirm the theoretical analysis carried out.

The choices of these two converters are as follows:

- The characteristics of the two converter topologies are very similar.
- They both use a capacitor as the main energy storage.
- They provide capacitive isolation which protects them against switch failure (unlike the buck topology) [9].
- The input current of the Ćuk and SEPIC topologies is continuous, and they can draw a ripple free current from a PV array which is important for efficient MPPT.
- The circuits have low switching losses and high efficiency [10].

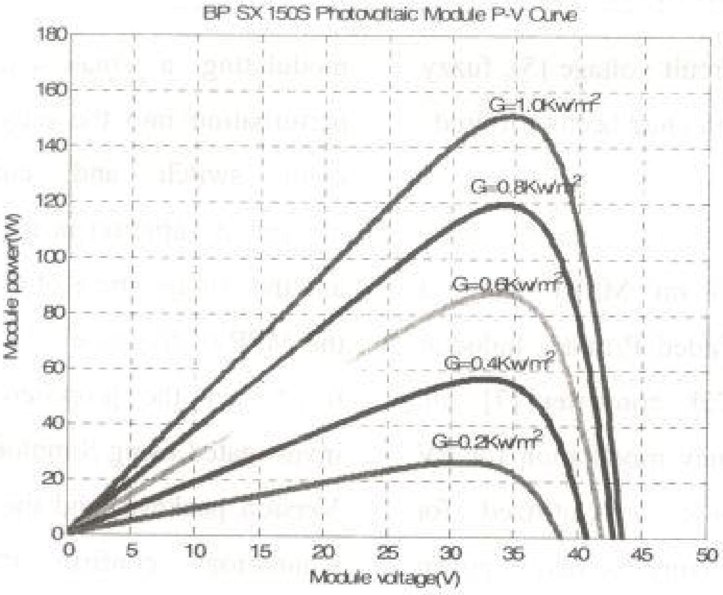


*Fig: 1 P-V curve for photovoltaic panel*

## *2.0 MODELING OF THE CONVERTER INPUT AT MPP*

The Thevenin's equivalent circuit of the solar panel connection to a converter is shown in Fig.2. The equivalent circuit of the solar panels often consists of a current source shunted by a diode and a resistor with an output series resistor [10].

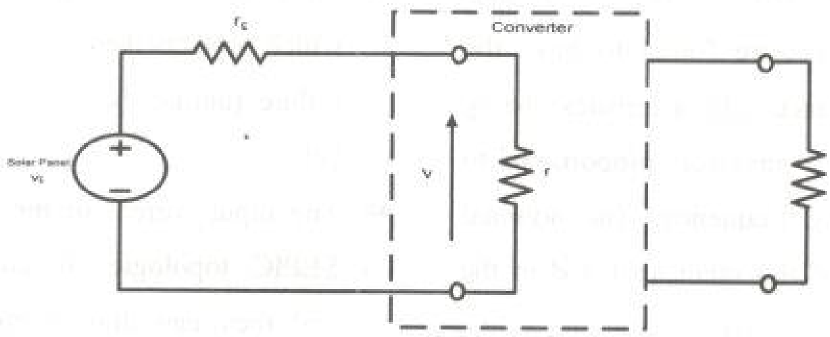


***Fig.2: Thevenin's equivalent circuit connecting converter***

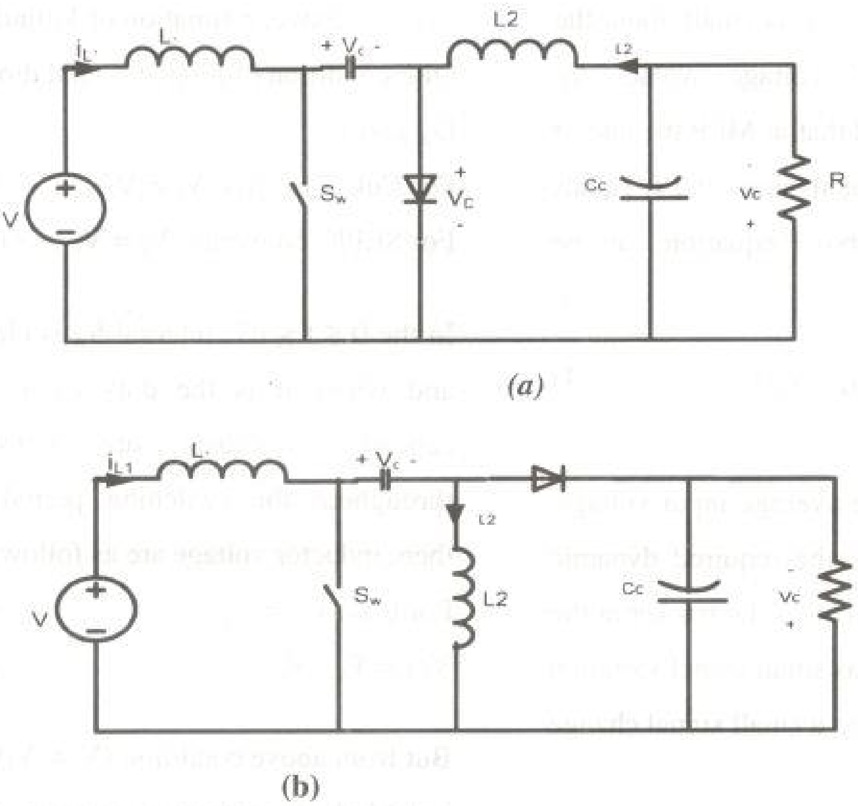


*Fig: 3 Circuit diagrams of (a) Ćuk and (b) SEPIC converter*

However, a Thevenin's equivalent circuit may be used to represent the solar panel at MPP in this case, which is made up of voltage source $v_g$ connected in series with an output resistance $r_g$. Where $v_i$ is the input voltage and $r_i$ is the equivalent input resistance of the converter. It is worthy to note that both $v_g$ and $r_g$ are subjected to the same level of radiation from the sun (insolation) and temperature.

In an ideal situation, where the converter is loss less, the input power $P_i$ into the tracker is equal to the output power $P_0$ of the solar panel. That is, Input power $P_i$ = output power $P_0$

$$P_i = P_O = \frac{v_i^2}{r_i} \qquad (1)$$

From (1), the partial derivative of input power with respect to input voltage $v_i$ and equivalent resistance $r_i$ of the converter yields thus;

$$\partial P_i = 2\frac{v_i}{r_i}\partial v_i - \frac{d(v_i^2)}{\partial r_i^2}$$

$$= 2\frac{v_i}{r_i}\partial v_i - \frac{v_i^2}{r_i^2}\partial r_i \qquad (2)$$

For maximum power transfer, this condition holds $r_i = r_g$

$$dP_i = 0$$

$$2\frac{v_i \partial v_i}{r_i} = \frac{V_i^2}{r_i^2}\partial r_i$$

$$\partial v_i = \frac{V_i}{2r_i}\partial r_i \qquad (3)$$

If the variation in $v_i$ is small about the average input voltage value $V_i$, bearing in mind that at MPP the rate of change of $P_i$ equals zero and $r_i$ equals $r_g$; then the above equation can be written as;

$$dv_i = \frac{V_i}{2r_i} dr_i, (r_i \approx r_g) \qquad (4)$$

Where $V_i$ is the average input voltage. Then, (4) gives the required dynamic input characteristic of the tracker at the MPP when $v_i$ has small signal variation of $\partial v_i$, subject to a small signal change of $\partial r_i$.

In Fig. 2 the converter that connects to the solar panel is either a Ćuk or SEPIC converter operating in discontinuous inductor current mode (DICM). The tracking operations for the above converter are described in the following section;

The basic assumptions that should be made before the analysis will be carried out are that $L_1$, $L_2$, $C$ and $C_o$ is large enough that $V_i$, $V_C$ and $V_o$ are *D.C* values, i.e. ripple free.

## 3. Discontinuous Inductor Current Mode (DICM) Operation

Since average value of voltage across each inductor $L$ is zero when referred to Fig.3 above, estimation of $V_c$ under OFF condition of Switch $S_w$ and diode $D_m$ gives;

For Ćuk converter, $V_c = V_i$ (5a)

For SEPIC converter, $V_c = V_i$ (5b)

In the $0 \leq t \leq dT_s$ interval $S_w$ is closed and where $d$ is the duty cycle, the capacitor voltages are constant throughout the switching period $T_s$, then, inductor voltage are as follows;

For Ćuk, $V_{L1} = V_i$ (6a)

$V_{L2} = V_c - V_o$ (6b)

But from above condition ($V_c = V_i$), input inductor current $i_{L1}$ is given as;

$$\frac{L_1 di_{L1}}{dt} = V_{L1} = V_i$$

$$i_{L1} = \frac{V_i}{L_1} t + I_1 \qquad (7)$$

Current through output inductor $i_{L2}$ is given as; $\frac{L_2 di_{L2}}{dt} = V_{L2} = V_i$

$$i_{L2} = \frac{V_i}{L_2} t - I_1 \qquad (8)$$

where $I_1$ is the initial current in $L_1$ when $D_m$ and $S_m$ are OFF.

For SEPIC: $V_{L1} = V_i$, $V_{L2} = V_c = V_i$

$$\frac{L_1 di_{L1}}{dt} = V_{L1} = V_i$$ (I.e. Current through input inductor $L_1$)

$$i_{L1} = \frac{V_i}{L_1} t + I_1 \qquad (9)$$

$$\frac{L_2 di_{L2}}{dt} = V_{L2} = V_i$$

$$i_{L2} = \frac{V_i}{L_2}t - I_1 \tag{10}$$

Observe that (8) and (10) are the same. Analyses were carried out for the remaining stages in the like manner and the summary of the results shown below.

$$i_{L1}(t) = \begin{cases} \frac{v_i}{L_1}(t) + I_1 & \text{for } 0 < t < dT_s \\ -\frac{v_i}{L_1}(t) + \frac{(v_i + v_o)}{L_1} dT_s + I_1 & \text{for } dT_s < t < (d+d_1)T_s \\ I_1 & \text{for } (d+d_1)Ts < t \le Ts \end{cases} \tag{11}$$

$$i_{L2}(t) = \begin{cases} \frac{v_i}{L_2}(t) - I_1 & \text{for } 0 < t < dT_s \\ -\frac{v_o}{L_2}t + \frac{(v_i + v_o)}{L_2} dT_s - I_1 & \text{for } dT_s < t < (d+d_1)T_s \\ -I_1 & \text{for } (d+d_1)Ts < t < Ts \end{cases} \tag{12}$$

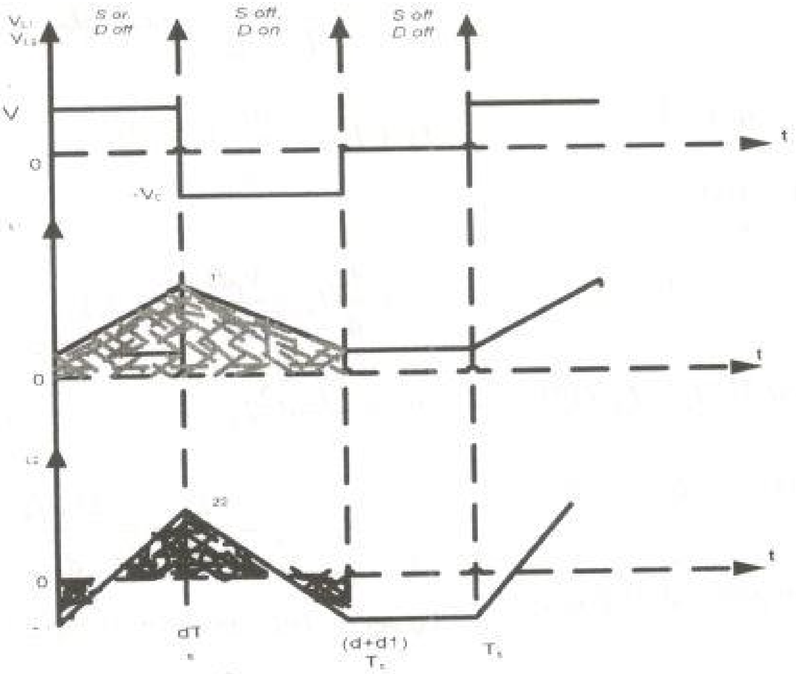


***Fig:4 Theoretical waveforms of $L_1$ and $L_2$ in DICM for Cuk & SEPIC converters***

### *4.0 Relationship between $V_i$ And $V_o$*

From the waveform of Fig.4 above, the average output voltage $V_{Lo}$ across the inductor is zero over a cycle.

$$V_{L0} = \frac{1}{Ts}\left[V_i dT_s - V_o(d + d_1 - d)T_s\right]$$

That yields, $V_i d - V_o d = 0$

$$\therefore \frac{V_o}{V_i} = \frac{d}{d_1} \tag{13}$$

Taking the average inductor output current $I_{Lo}$, i.e. the shaded portion $I_{L1}$ of the above waveform, will give us thus;

Since $I_{L1o}$ = average of $I_{L1}$

$$I_{L10} = \int_0^{Ts} I_{L1} dt$$

$$I_{L10} = \frac{1}{T_s}\left[I_1 T_s + \frac{1}{2}(I_{11} - I_1)(d + d_1)T_s\right]$$

$$I_{L10} = I_1 + \frac{V_i dT_s}{2L_1}(d + d_1) = I_s \quad (14)$$

Secondly, the average of $I_{L2}$ equals inductor 2 output current $I_{L2o}$. The shaded portion of Fig. 3 gives $I_{L2}$.will give thus, $I_{L2o}$ = average of $I_{L2}$

$$I_{L20} = \frac{1}{T_s}\left[\frac{1}{2}(I_{22} + I_1)(d + d_1)T_s - I_1(d + d_1)T_s - I_1(T_s - (d + d_1)T_s)\right]$$

Canceling Ts and all other like terms yield

$$= \frac{1}{2}(I_{22} + I_1)(d + d_1) - I_1$$

where $I_{22}$ $[(V_i dT_s/2L_2) - I_1 + I_1]$

$$= \left(\frac{V_i dT_s}{2L_2} - I_1 + I_1\right)(d + d_1) - I_1$$

$$I_{L20} = \frac{V_i dT_s}{2L_2}(d + d_1) - I_1 = I_0 \quad (15)$$

$P_i = V_i * I_{L1o} = V_i * I_s$ where $I_s$ is the average source current.

Similarly, the output power $P_o$ is given by;

$P_o = V_o * I_{L2o} = V_o * I_o$ where $I_o$ is the average output current.

This analogy is also applicable to SEPIC converter.

Considering only Ćuk converter, using the power balance, we have,

$$V_i I_1 = V_o I_o \quad (16)$$

Eliminating $V_o$ from (16) and (13), yields thus;

$$V_i I_1 = I_0 * \frac{V_i d}{d_1}$$

$$\therefore I_0 = \frac{d_1}{d} I_s \quad (17)$$

Adding (12) and (13), we arrived that

$$I_0 + I_s = \frac{V_i dT_s}{2}(d + d_1)\left(\frac{1}{L_1} + \frac{1}{L_2}\right) \quad (18a)$$

Taking a look at Fig.3 the converter circuit diagrams $L_1$ and $L_2$ are in parallel

$$\therefore L_r = \frac{L_1 * L_2}{L_1 + L_2} \quad i.e. L_1 \| L_2$$

$$I_0 + I_s = \frac{V_i dT_s}{2L_r}(d + d_1)$$

Then,

$$I_s + \frac{d_1}{d} I_s = \frac{V_i dT_s}{2L_r}(d + d_1)$$

$$I_s = \frac{V_i}{2L_r} d^2 T_s \quad (18b)$$

$$\frac{V_i}{I_s} = R_i = r_i = \frac{2L_r}{d^2 T_s} = \frac{2L_r f_s}{d^2} \quad (19)$$

To get $d_1$, one can consider input and output power of

$$V_i I_{Li} = \frac{V_o^2}{R} \quad (19b)$$

Substituting (18b) into (19b) and using voltage conversion ratio $M = V_o/V_i = d/d_1$

That gives; $d_1 = \sqrt{2L_r f_s / R}$ (19c)

From the diagrams of Fig.3, we can deduce that the condition for DICM is as follows:

$$T_s > (d + d_1)\, T_s$$

$$1 > d + d_1$$

$$1 - d_1 > d \qquad (20)$$

Voltage stress on switch *Sw* is when *Sw* is off and D is on while voltage stress on diode D is when Sw is on and D is off for SEPIC

$$V_{Sw.stress} = V_{Dstress} = V_o + V_c \qquad (20b)$$

But for cuk $V_{Swstress} = V_{Dstress} = V_c$ (20c)

After substituting (5a) into (20c) and (5b) into (20b), it was found that

$$V_{Swstress} = V_{Dstress} = (1+M)V_i$$

$$= \left(1 + \frac{d}{\sqrt{2L_r f_s / R}}\right) V_i \qquad (20d)$$

Equation (20d) is the same for both converters.

By differentiating (19) with respect to $f_s$, it can be seen that a small change of $f_s$ will introduce a small variation in $r_i$. Hence,

$$\frac{\partial r_i}{\partial f_s} = \frac{2L_r}{d^2}$$

$$\partial r_i = \frac{2L_r \partial f_s}{d^2} \qquad (21)$$

Therefore, injecting a small sinusoidal variation into fs gives;

$$f_s = \overline{f}_s + \partial f_s$$

$$f_s = \overline{f}_s + \hat{f}_s \sin(2 f_m t) \qquad (22)$$

where $\overleftarrow{fs}$ is nominal switching frequency, $f_m$ is the modulating frequency and is much lower than the nominal switching frequency, $\hat{fs}$ is the maximum frequency deviation.

Thus, with the above switching frequency perturbation, $\boldsymbol{r_i}$ will include an average resistance $\boldsymbol{R_i}$, and a small variation $\partial \boldsymbol{r_i}$, thereby gives;

$$r_i = R_i + \partial r_i$$

where $R_i = \frac{2L_r}{d^2} \bar{f}_s$ and

$$\partial r_i = \frac{2L_r}{d^2} \hat{f}_s \sin(2\pi f_m t)$$

Let us assume that $D_{mpp}$ be the required duty cycle of the switch $S_m$ at MPP. Then, $r_g$ can be expressed as;

$$r_g = \frac{2L_r}{D^2_{mpp}} \overline{f}_s \qquad (23)$$

Applying voltage divider to Fig. 2

$$V_i = \frac{(R_i)}{R_i + r_g} v_g \qquad (24)$$

Substituting the value for $R_i$ and $r_g$ into (24) yields

$$Vi = \frac{D^2_{mpp}}{D^2_{mpp} + d^2} v_g \qquad (25)$$

Similarly, considering the small-signal variation of $v_i$ with respect to $r_i$ yields

$$\partial v_i = \frac{d}{dri}\left(\frac{r_i}{r_i + r_g} v_g\right) \partial r_i$$

$$\partial v_i = \left(\frac{r_g}{(R_i + r_g)^2} v_g\right) \partial r_i \qquad (26)$$

Substituting the value for $\delta r_i$, $R_i$ and $r_g$ into (26) gives;

$$\partial v_i = \frac{\left(D^2{}_{mpp} * d^2\right) v_g}{(D^2{}_{mpp} + d^2)^2 \bar{f}_s} \partial fs \qquad (27)$$

The peak value of $\partial v_i$ i.e. $\bar{v}$ and bearing in mind that $\partial fs$ gives $\hat{f}_s \sin(2 f_m t)$ and at MPP the maximum frequency deviation $\hat{f}_S$ is used.

$$\bar{v}_i = \frac{\left(D_{mpp} * d\right)^2 * v_g}{\left(D^2{}_{mpp} + d^2\right)^2 \bar{f}_s} \hat{f}s \qquad (28)$$

As $V_g$ and $r_g$ vary with insolation and temperature, $d$ should be automatically adjusted to $D_{mpp}$ in the controller. By substituting the values of the forgoing $\partial r_i$ and $Ri$, into (4), since $r_i = r_g$, the equation obtained holds at the MPP.

$$\partial v_i = \bar{v}_i = \frac{\hat{f}s}{2\bar{f}_s} V_i \qquad (29)$$

Comparing (25) with (28), the difference between the normalized characteristics of $\hat{f}s V_i / 2\bar{f}s v_g$ and $\bar{v}_i / v_g$ ,(that is the value of input stead state voltage Vi with small-signal variation of input voltage $\bar{v}_i$), will yield

$$\varepsilon_1(k) = \frac{\hat{f}s V_i}{2\bar{f}_s v_g} - \frac{\bar{v}_i}{vg}, \quad \text{but let}$$

$$\beta = \frac{\hat{f}s}{2\bar{f}_S} = \beta \frac{V_i}{v_g} - \frac{\bar{v}_i}{v_g}$$

Substituting (25) and (28) into the above equation gives

$$\varepsilon_1(k) = \beta\left[\frac{D^2{}_{mpp}}{D^2{}_{mpp} + d^2}\right] - 2\beta\left[\frac{(D_{mpp} d)^2}{\left(D^2{}_{mpp} + d^2\right)^2}\right]$$

Let K = d/$D_{mpp}$

$$\varepsilon_1(k) = \beta\left[\frac{1 - k^2}{\left(1 + k^2\right)^2}\right] \qquad (30)$$

Where $k = \dfrac{d}{D_{mpp}}$ and $\beta = \dfrac{\hat{f}s}{2\bar{\bar{f}}s}$

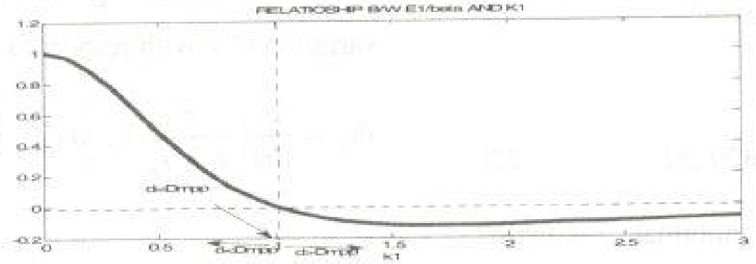


*Fig. 5: Relationship between $\varepsilon_1/\beta$ & $k_1$*

By critically looking at the graph of fig.5, we can deduce the following points;

If $d < D_{mpp}$ (i.e. $K < 1$), $\varepsilon_{1(k)} > 0$ (31a)

If $d = D_{mpp}$ (i.e. $K = 1$), $\varepsilon_{1(k)} = 0$ (31b)

If $d > D_{mpp}$ (i.e. $K > 1$), $\varepsilon_{1(k)} < 0$ (31c)

From the Fig.5, the difference between the value of input stead state voltage Vi with small-signal variation of input voltage $\overline{v}_i$, which is ($\varepsilon$) when subjected to switching frequency perturbation if plotted against tracking duty-cycle of the converter, which tracks the maximum power of the PV at point where switch duty-cycle $d$ is equals $D_{mpp}$, which is the required duty cycle of the switch at MPP. If the $d$ is less than $D_{mpp}$ then the system will not work favourablly. This confirms the earlier statement that as $\boldsymbol{v_g}$ and $\boldsymbol{r_g}$ vary with insolation and temperature, $d$ should be automatically adjusted to $D_{mpp}$ in the controller until both duty cycles were equal. By then controller would have tracked the maximum point of the PV.

## 5.0 *SIMULATION RESULTS FOR DICM*

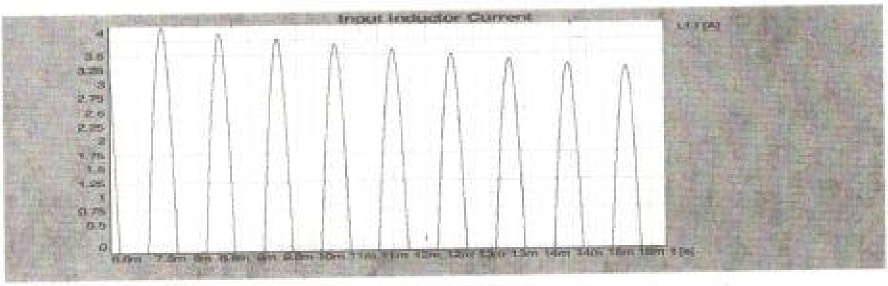


**(a)**

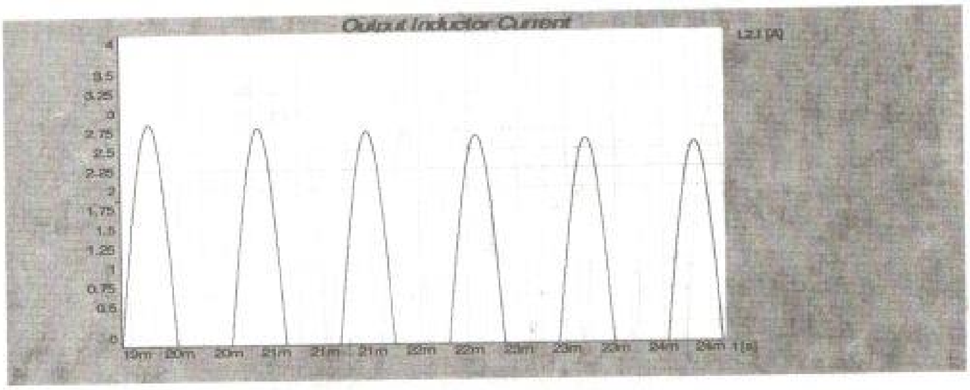


***(b)***

***Fig. 6: Ćuk DICM operation (a) $L_1$, (b) $L_2$ current***

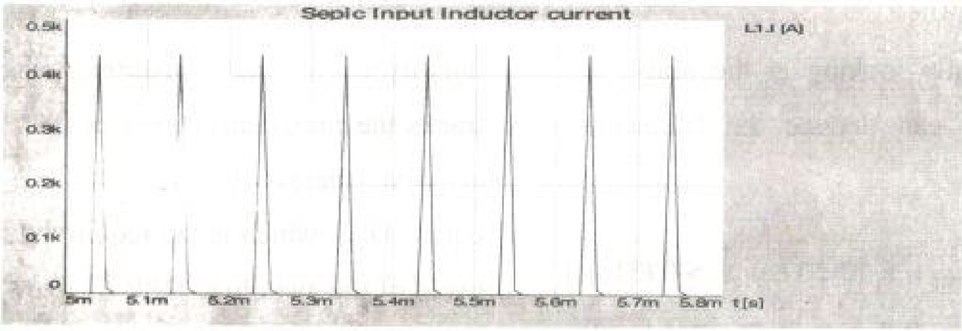


(a)

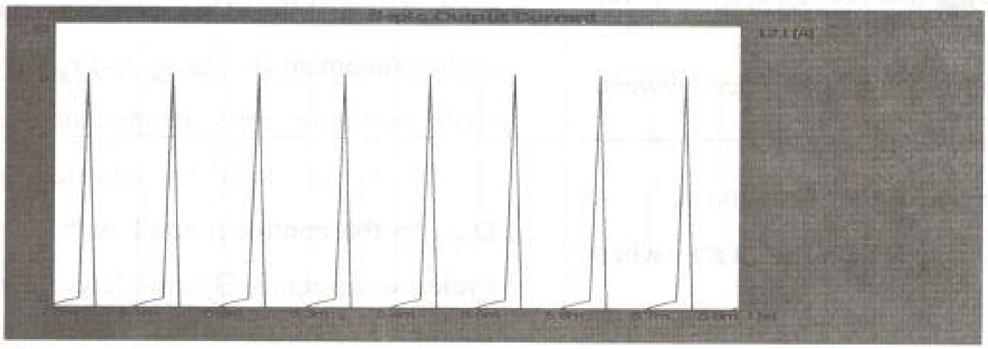

(b)

*Fig 7: SEPIC converter DICM operation (a) $L_1$ & (b) $L_2$*

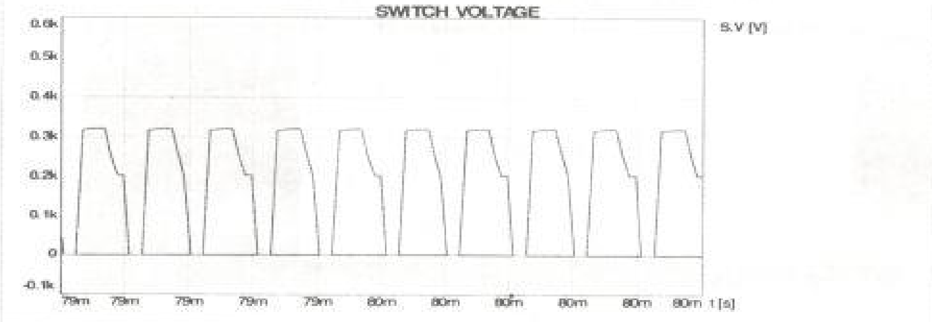


*Fig 8: Voltage Stress of the switch*

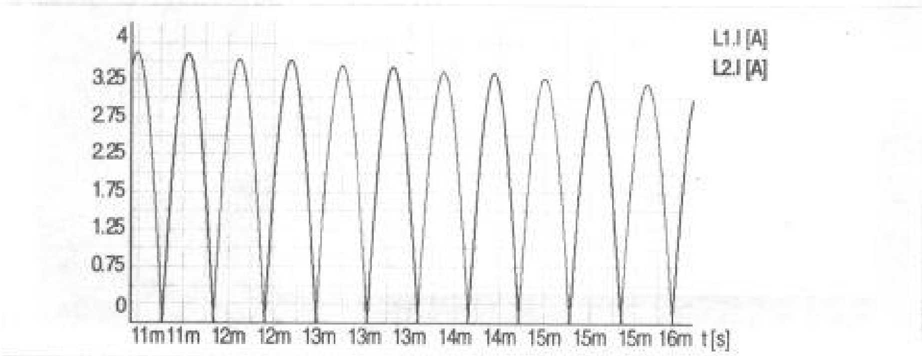


*Fig:9: Ćuk converter currents across inductors $L_1$ & $L_2$*

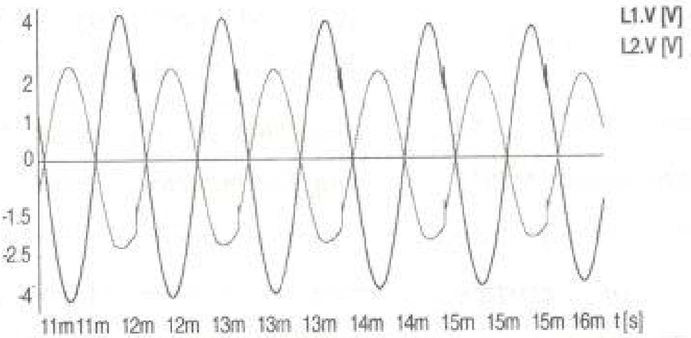


*Fig.10: Voltages across inductors $L_1$ & $L_2$ respectively*

## *6.0* Analysis of Simulation Results

The simulations were done in Simplorer 6.0 student version using the different inductors values for both converters in DICM operation. From the simulation results of both converters, it is observed that input inductor current $i_{L1}$ for both converters are discontinuous confirming the analytical results. Secondly, output inductor currents $i_{L2}$ for both converters are also discontinuous as expected. A look at Fig: 9 shows the two inductors currents in one graph, from the result one can appreciate the operations of the two inductors interchangeably. When $i_{L1}$ goes discontinuous, then $i_{L2}$ starts to charge.

Also, from Fig: 10, one can observe that as $i_{L1}$ is discharging, $i_{L2}$ is charging and vice versa. Similarly, Fig .8 shows the effect of voltage stress on the active switch. The simulation results validate the theoretical analysis done so far. Similarly, MATLAB software package was equally used to run some programs that confirm that the analysis done was in order.

## 7.0 CONCLUSION

A switching frequency modulation for maximum power point tracking techniques has been presented. A PWM dc-dc Ćuk or SEPIC converter operating in discontinuous inductor-current mode was used to match with the output resistance of the solar panel.

A small-signal sinusoidal perturbation was injected into the switching frequency and the result compared favourably with the average value of the panel terminal voltage and the ac components variation of the input voltage. With this procedure the maximum power point can then be located.

**REFFERENCE**

[1]. J. Yu, Y.S. Jung, J.Y. Choi, and G. S. Kim, "*A novel two-mode MPPT Control* Algorithm *based on comparative study of existing algorithms*", available online at www.sciencedirect.com

[2] Dezso Sera, Remus Teodorescu,Tamas Kerekes, "*Teaching Maximum Power Point Trackers Using a PV Array Model with Graphical User Interface*"available online at www.highbeam.com

[3] M. Belarbi, K. Haddouche, A. Midoun, "*Modeling and simulation of photovoltaic solar panel*", *WREEC* 2006 .

[4] Mohmmad A.S Masoum, Hooma Dehbnei, and Ewald f, Fuchs, "*Theoretical and Experimental Analyses of Photovoltaic Systems with Voltage- and Current-Based Maximum Power Point Tracking*", IEEE Trans.on Energy conv. Vol.17, no 4. Dec.2002

[5] J. J. Schoeman and J. D. van Wyk,"*A simplified maximal power controller for Terrestrial photovoltaic panel arrays,*" in 13th Annual IEEE Power Electron. Specialists Conf., 1982, pp. 361-367.

[6] M. Veerachary, T. Senjyu, and K.Uezato,"*Neural-network-base maximum Power point tracking of coupled-inductor interleaved boost converter-supplied PV system using fuzzy controller,*" IEEE Trans. Ind. Electron., vol. 50, pp. 749- 758, Aug. 2003

[7] K.K Tse, M. T. Ho, Henry S. H Chung and S.Y. (Ron) Hui, "*A Novel MPPT for PV Panels Using Switching Frequency Modulation*", IEEE Trans. Power Electronics, Vol. 17, no. 6. Nov. 2002

[8] Henry Shu-Hung chung, K. K. Tse, S. Y. Ron Hui, C. M. Mok, and M. T. Ho, "*A Novel MPPT Technique for Solar Panels Using a Sepic or Cuk Converter*", IEEE Trans. On Power Electronics Vol. 18, no. 3. May 2003

[9] Hohm, D. P. & M. E. Ropp, "*Comparative Study of Maximum Power Point Tracking* Algorithms" Progress in Photovoltaic: Research and Applications November 2002, page 47-62

[10] Rashid, Muhammad H. "*Power Electronics - Circuits, Devices, and Applications*" *3rd Edition* Pearson Education, 2004